Journal of Sound and Vibration (1994) **176**(3), 399–413

ACOUSTIC PROPERTIES OF FLUID-FILLED ELASTIC PIPES

L. FENG

Department of Technical Acoustics, Royal Institute of Technology, S-100 44 Stockholm, Sweden

(*Received* 14 *July* 1992, *and in final form* 3 *May* 1993)

The acoustic properties of an infinite, fluid-filled pipe have been investigated. The relation between radiated sound power and the system power distribution for a single mode is analyzed. Energy flow is examined. Coupling effects on acoustic properties are compared. Whether coupling with fluid will increase or decrease pipe response, and hence noise power, is largely dependent on the frequency range and on the method of excitation.

1. INTRODUCTION

During recent years, great attention has been paid to coupled fluid–pipe systems. Fuller and Fahy [1] performed a thorough analysis of dispersion relations and energy distributions for a single mode travelling in a fluid-filled elastic pipe. Pavic investigated vibrational energy flow in straight pipes for two cases, *in vacuo* and fluid-filled [2, 3]. Pavic also described the intereference of different travelling modes with the same circumferential distributions. The pipe response to an external force exciting the pipe wall was analyzed by Fuller [4]. In this reference the "power ratio" is in fact at the source plane, which is usually the minimum of the ratio. In references [5, 6], Fuller described the fluctuation of radiated sound along the axial distance for symmetric modes, introducing the concept of "surface power", which constitutes an axial energy flow but never contributes to the radiated far field.

This paper is concerned with the relations between the structure and the resulting acoustic fields, and the coupling influence on the acoustic properties of the system. A method similar to that of references [1, 4] is used to determine the qualities of a straight, infinite elastic pipe filled with fluid. Damping is not included. An internal fluid – external vacuum model is employed to calculate dispersion curves, power distributions and pipe responses to applied external forces. The displacements obtained are then utilized to calculate the radiated acoustic fields, providing a good approximation for a pipe filled with a heavy fluid, vibrating in air, but not applicable if surrounded by a dense fluid. Simple harmonic wave motion is considered throughout the paper. The factor $\exp(j\omega t)$ is omitted in all of expressions shown. In calculations of pipe responses and acoustic fields, only travelling waves are taken into account.

2. GENERAL PROPERTIES

The co-ordinate system is shown in Figure 1. The motion of a thin walled cylindrical shell can be described by the simplified Flügge equations [7]

0022–460X/94/380399 + 15 $08.00/0

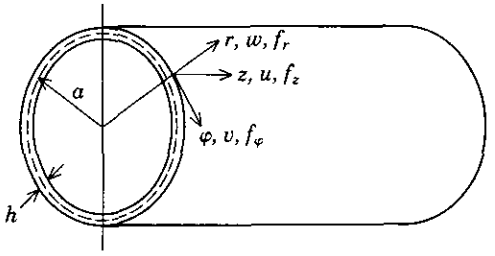

Figure 1. The co-ordinate system.

$$\frac{w}{a^2}+\beta^2\left(a^2\frac{\partial^4}{\partial z^4}+2\frac{\partial^4}{\partial\varphi^2\,\partial z^2}+\frac{1}{a^2}\frac{\partial^4}{\partial\varphi^2}\right)w+\frac{1}{a^2}\frac{\partial v}{\partial\varphi}+\frac{\nu}{a}\frac{\partial u}{\partial z}-\frac{(f_r+p)}{\rho_s h c_s^2}=-\frac{1}{c_s^2}\frac{\partial^2 w}{\partial t^2},$$

$$\frac{1}{a^2}\frac{\partial w}{\partial\varphi}+\left(\frac{1}{a^2}\frac{\partial^2}{\partial\varphi^2}+\frac{1-\nu}{2}\frac{\partial^2}{\partial z^2}\right)v+\frac{1+\nu}{2a}\frac{\partial^2 u}{\partial\varphi\,\partial z}+\frac{f_\varphi}{\rho_s h c_s^2}=\frac{1}{c_s^2}\frac{\partial^2 v}{\partial t^2},$$

$$\frac{\nu}{a}\frac{\partial w}{\partial z}+\frac{1+\nu}{2a}\frac{\partial^2 v}{\partial\varphi\,\partial z}+\left(\frac{\partial^2}{\partial z^2}+\frac{1-\nu}{2a^2}\frac{\partial^2}{\partial\varphi^2}\right)u+\frac{f_z}{\rho_s h c_s^2}=\frac{1}{c_s^2}\frac{\partial^2 u}{\partial t^2}. \tag{1}$$

In these equations, a is the pipe mean radius, ν is the Poisson ratio, $c_s=\sqrt{E/(1-\nu^2)\rho_s}$ is the plate extensional wave speed, E is Young's modulus, ρ_s is the density of the pipe material, ω is the angular frequency, h is the pipe thickness, $\beta^2=h^2/12a^2$, p is the acoustic pressure in the fluid, w, v, u and f_r, f_φ, f_z are displacements and external forces (unit area, dimension $[\mathrm{ML}^{-1}\mathrm{S}^{-2}]$) applied to the pipe in the r, φ, and z directions, respectively. (A list of symbols is given in Appendix B).

The solutions of equation (1), in discrete form, can be expressed as

$$\begin{bmatrix}w(\varphi,z)\\v(\varphi,z)\\u(\varphi,z)\end{bmatrix}=\sum_{n=0}^{\infty}\begin{bmatrix}w_n(z)\cos(n\varphi)\\v_n(z)\sin(n\varphi)\\\mathrm{j}u_n(z)\cos(n\varphi)\end{bmatrix}=\sum_{n=0}^{\infty}\sum_{m=1}^{\infty}\begin{bmatrix}w_{nm}\cos(n\varphi)\\v_{nm}\sin(n\varphi)\\\mathrm{j}u_{nm}\cos(n\varphi)\end{bmatrix}\mathrm{e}^{-\mathrm{j}k_{nm}z},\qquad z>0, \tag{2}$$

where k_{nm} is the axial wavenumber of the mode (n, m). It is assumed that the excitation is symmetric about $\varphi=0$.

The wave motion in the fluid is described by a linear acoustic equation, solved by a combination of cosine and Bessel functions. These two solutions are matched together by setting the radical particle velocities in the two media to be the same at the wall, leading to the characteristic equation as

$$x_n\mathrm{J}_n'(x_n)L_1(y_n)=\eta\Omega^2\mathrm{J}_n(x_n)L_2(y_n), \tag{3}$$

where the subscript n refers to the circumferential distribution $\cos(n\varphi)$, $\Omega=wa/c_s$ is the normalized frequency, J_n is the Bessel function of order n, $y_n=k_n a$ is the normalized axial wavenumber, and $x_n=\sqrt{[\Omega^2(c_s/c_f)^2-y_n^2]}$ is the normalized radial wavenumber in the fluid. The subscript f denotes "fluid", a prime denotes differentiation with respect to the argument, and

$$L_1(y_n)=\frac{1-\nu}{2}(1-\nu^2-\Omega^2)y_n^4-\left[\frac{(3-\nu)(1-\Omega^2)}{2}+(1-\nu)n^2-\nu^2\right]\Omega^2y_n^2$$
$$+\left(\Omega^2-\frac{1-\nu}{2}n^2\right)(1+n^2-\Omega^2)\Omega^2+\beta^2(n^2+y_n^2)^2L_2(y_n), \tag{4}$$

$$L_2(y_n)=(y_n^2+n^2-\Omega^2)\left(\frac{1-\nu}{2}(y_n^2+n^2)-\Omega^2\right). \tag{5}$$

The coupling parameter η in equation (3) is

$$\eta = \frac{\rho_f a}{\rho_s h} \simeq 2 \cdot \frac{\text{unit length fluid mass}}{\text{unit length shell mass}}. \tag{6}$$

The physical meaning of equation (3) is very clear: the pipe vibrating *in vacuo* ($L_1(y_n) = 0$) and the acoustic wave in a rigid walled duct ($x_n J_n'(x_n) = 0$) are coupled together via a variable coupling coefficient $\eta\Omega^2 J_n(x_n) L_2(y_n)$, the magnitude of which depends on the particular wave mode concerned. There is no coupling when η equals zero.

Fuller has demonstrated [8] that there is a flow of energy backward and forward between the pipe and fluid as the wave field propagates down the fluid–pipe system. He concluded that this is due to the cross terms of the non-orthogonal modes. If the analogies of y_n to ω and z to t are taken, the form of equation (3) is the same as that of the equation of coupled oscillators. From the properties of coupled oscillators [9], this phenomenon of energy transfer along the z-axis can immediately be expected. The density of the fluid (represented by the coupling parameter η) only changes the strength of the energy transfer, but does not determine whether or not the phenomenon will occur.

3. POWER RATIO FOR A SINGLE MODE

The term "power ratio" here means the ratio of sound power radiated by a unit length of the pipe divided by vibrational energy flow through a cross section.

The time averaged axial energy flow of a unit width of a thin walled cylindrical shell can be written as [10]

$$\bar{P}_z = -\left\{\overline{\dot{w}Q_z} + \overline{\dot{v}N_{z\varphi}} + \overline{\dot{u}N_z} + \overline{\left(\frac{1}{a}\frac{\partial \dot{w}}{\partial \varphi} - \frac{\dot{v}}{a}\right)M_{z\varphi}} + \overline{\frac{\partial \dot{w}}{\partial z} M_z}\right\}, \tag{7}$$

where an overdot implies differentiation with respect to time and an overbar denotes time averaging. Q_z, N_z, $N_{z\varphi}$, $M_{z\varphi}$ and M_z are the transverse shear force, axial force, torsional shear force, shear moment and bending moment respectively.

The acoustic intensity for harmonic wave motion in the axial direction is given by

$$I_z^f = \tfrac{1}{2}\,\mathrm{Re}\,(pu_z^{f*}), \tag{8}$$

where the superscript f denotes "fluid" and the asterisk denotes the complex conjugate.

Energy flow through any cross-section of the wall is the integral of expression (7) over the circumference, and acoustic energy flow is the integral of expression (8) over the cross-section. The total energy flow is the sum of these two. By using simplified Flügge equations [7], for the mode (n, m) it is obtained as (see Appendix A)

$$\begin{aligned} T_{znm} = T_{znm}^s + T_{znm}^f = \frac{\epsilon_n \pi \rho_s c_s^3 \Omega h}{2a}\Bigg\{&\left(y_{nm} R_u^2 + \nu R_u + \frac{1+\nu}{2} n R_u R_v + \frac{1-\nu}{2} y_{nm} R_v^2\right) \\ &+ \beta^2 y_{nm}(2n^2 + 2y_{nm}^2 + n R_v) \\ &+ \eta \frac{\Omega^2 y_{nm}}{2x_{nm}^2 J_n'^2(x_{nm})}\left[\left(1 - \frac{n^2}{x_{nm}^2}\right) J_n^2(x_{nm}) + J_n'^2(x_{nm})\right]\Bigg\} w_{nm}^2, \end{aligned} \tag{9}$$

where $\epsilon_n = 2$ if $n = 0$ and $= 1$ if $n \neq 0$. R_u and R_v are displacement ratios, defined as

$$R_u = \frac{u_{nm}}{w_{nm}} = \frac{y_{nm}}{L_2(y_{nm})}\left(\frac{1-\nu}{2} n^2 - \frac{\nu(1-\nu)}{2} y_{nm}^2 + \nu\Omega^2\right), \tag{10}$$

$$R_r = \frac{v_{nm}}{w_{nm}} = \frac{n}{L_2(y_{nm})}\left(\Omega^2 - \frac{1-\nu}{2}(n^2 + y_{nm}^2) - \frac{1-\nu^2}{2}y_{nm}^2\right). \tag{11}$$

Note that $R_r = 0$ when $n = 0$, since the torsional mode is decoupled for axisymmetric motion.

The radiated sound power can be approximated by using the radial displacement obtained from the previous model when the pipe is surrounded by air. It is easy to prove that (see equations (17)–(23) in the later part of the paper, with $K_n = 1$), for the mode (n, m), the sound power radiated by a unit length (length a) of a vibrating pipe is

$$T_{nm}^a = \frac{\epsilon_n \pi a^2 \rho_a c_a \omega^2 \sigma_{nm}}{2} w_{nm}^2, \tag{12}$$

where subscript and superscript a denotes air, and σ_{nm} is the radiation efficiency of mode (n, m) as defined in reference [11]. Radiation efficiencies for different modes have been examined in reference [12], where it was found that the discrepancies between different modes with the same circumferential distribution are usually less than 0·5 dB, and between different circumferential distributions show the same properties as in reference [11].

The relation between radiated noise power and different parts of structure energy flow is examined. In order to do this, five different types of power ratios are calculated. Their definitions are as follows:

$$\Gamma_q = 10 \log \frac{\text{sound power radiated per unit length}}{\text{energy flow type } q}, \quad q = f, s, b, e, t. \tag{13}$$

Here the subscript f denotes "fluid" (terms with η), s "shell" (terms without η), b "bending" (terms with β^2), e "extension" (terms without β^2 and η) and t "total energy

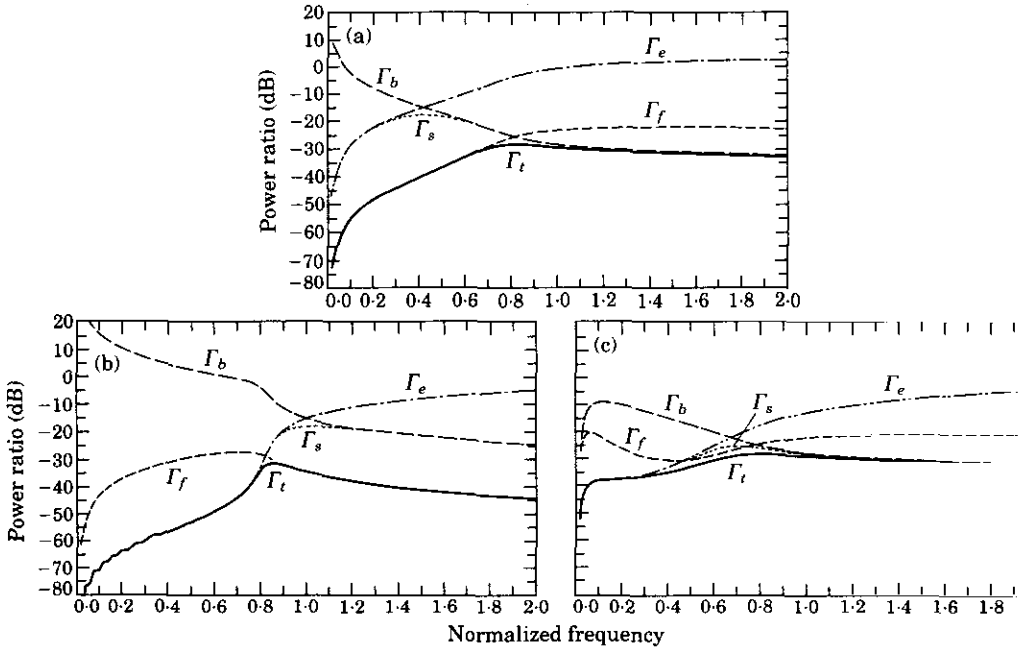

Figure 2. Power ratios for single travelling mode. Water/steel pipe system, $h/a = 0{\cdot}05$. (a) (0, 1) mode; (b) (0, 2) mode; (c) (1, 1) mode.

TABLE 1

Geometrical and material parameters

Material	Poisson ratio, ν	Density, ρ (kg/m^3)	Free wave speed, c (m/s)
Steel	0·3	7800	5200
Water	—	1000	1500

Thickness ratio $h/a = 0{\cdot}05$.

flow". Among them, Γ_t is the measure of how much structural power is needed to radiate a certain amount of noise power. Similarly, other partial power ratios, i.e., Γ_f, Γ_s, Γ_b and Γ_e, are relations between radiated sound power and the several specific types of structure power. The ratios also show the power distribution in the system.

Various power ratios of the (0, 1), (0, 2) and (1, 1) modes are shown in Figure 2, with material parameters in Table 1. The ratios for any $(n, 1)$ mode with $n > 1$ are similar to those of the (1, 1) mode, and become more and more like each other with increasing circumferential number [12]. It is seen from the figure that the (0, 1) mode is the main radiation mode for axisymmetric motion, since the total power ratio Γ_t of the mode is much higher than that of the (0, 2) mode at all frequencies. Although vibrational energies of all principal radiation modes ($(n, 1)$ modes) for any circumferential distribution $\cos(n\varphi)$ with $n > 0$ are mainly propagating in the pipe, the situation for $n = 0$ is opposite: the main power of the (0, 1) mode is in the fluid when $\Omega < 1$, but it radiates much more noise than the (0, 2) mode, which is a shell mode, at the same frequencies. There seems to be no definite relation between radiated sound power and the energy distribution in the system. This result is not surprising, since the sound field is related only to the pipe radial velocity, but the energy flow in the shell contains three-dimensional vibration energy. A further examination of Figure 2 shows that there is even no definite relation between shell bending energy and the radiated noise power.

The negative of Γ_f, which corresponds to the ratio of fluid power to radiated sound power, is defined as transmission loss in reference [5]. This quantity is very dependent on what modes are excited. As shown in Figure 2, the transmission loss of the (1, 1) mode (or any other non-axisymmetric mode) is at least 30 dB smaller than those of the breathing modes at low frequencies. The total transmission loss will drop dramatically if any non-axisymmetric mode is excited, as expected [5]. A difference from reference [5], however, is that the pipe and fluid are strongly coupled here. The fluid power varies appreciably with the axial distance if the frequency is high enough, as mentioned in the last section. In the author's opinion, it is more physically meaningful to use the total power ratio Γ_t rather than the transmission loss if the medium inside the pipe is a heavy fluid such as water. The comparison of the total power ratios Γ_t of several modes is shown in Figure 3. The ratio of mode (0, 2) is always lower than that of any of the others by at least 10 dB except close to $\Omega = 0{\cdot}8$ when the mode (0, 3) cuts on. As at low frequencies, this is a shell extensional mode, and at high frequencies this is a fluid plane wave mode. The shell radial displacement is very small in both cases. Hence this mode can always be neglected in practical noise control problems. The $n = 1$ mode is the most important only when $\Omega < 0{\cdot}08$. After that, the power ratios of $n = 2$, $n = 3$, $n = 4$, etc., surpass that of $n = 1$. At these frequencies, there is no reason to describe any particular mode as being most important unless the excitation is known. When the frequency is increased further, all of the different circumferential distributions have the same importance.

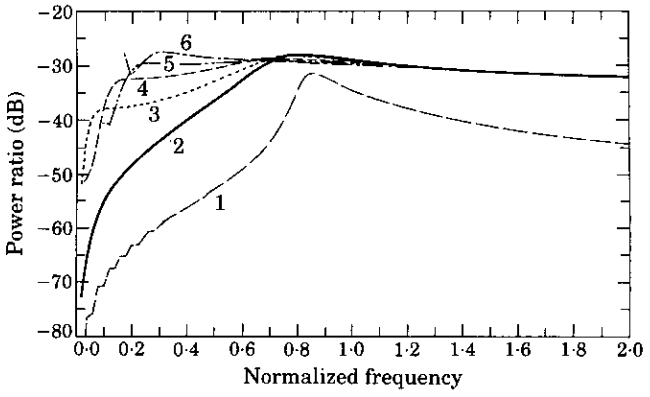

Figure 3. A comparison of the modal total power ratio Γ_i. Water/steel pipe system, $h/a = 0{\cdot}05$. 1, (0, 2) mode; 2, (0, 1); 3, (1, 1); 4, (2, 1); 5, (3, 1); 6 (4, 1).

4. FLUCTUATION ALONG THE AXIAL DIRECTION

Only external force excitation is considered here. Fluid excitation of the pipe may be approximated by an external force with a certain distribution, as viscosity is not included and the fluid excitation is only in the radial direction. As mentioned in the introduction, only travelling waves, i.e., the real roots of equation (3), will be taken into account.

4.1. VELOCITY DISTRIBUTION

Suppose that the external force applied to the pipe is uniformly distributed around the origin and is of the form

$$f_r(\varphi, z) = \begin{cases} F_0/(a\varphi_0 B), & |z| \leqslant B/2, \quad |\varphi| \leqslant \varphi_0/2 \\ 0, & \text{otherwise} \end{cases}, \tag{14}$$

where F_0 is the magnitude of the total applied force, B is the axial length of the distributed force and φ_0 is the angle of arc of the distribution. Except in the discussion of the coupling effects (section 5), point force excitation, i.e., the case in which $B = 0$ and $\varphi_0 = 0$, is applied to all of the calculations shown below.

By using the same approach as in reference [4], the radial velocity for each circumferential distribution $\cos(n\varphi)$, at the angle $\varphi = 0$, can be obtained as

$$\dot{w}_n\left(\frac{z}{a}\right) = \frac{\Omega F_0}{\rho_s c_s \pi a h \epsilon_n} \sum_{m=1}^{K_n} \frac{\sin(y_{nm} B/2a)}{y_{nm} B/2a} \cdot \frac{L_2(y_{nm})\, e^{-j(z/a)y_{nm}}}{[L_1(y_{nm}) - FL \cdot L_2(y_{nm})]'}, \qquad z \geqslant B/2, \tag{15}$$

where the prime denotes the derivative with respect to the argument, K_n is the total number of travelling waves with circumferential distribution $\cos(n\varphi)$, y_{nm} is the normalized wavenumber of the mode (n, m), and $FL = \eta\Omega^2 J_n(x_{nm})/x_{nm} J_n'(x_{nm})$ is the so-called "fluid loading term". The total velocity of the shell is then expressed as

$$\dot{w}(\varphi, z/a) = \sum_{n=0}^{\infty} \frac{\operatorname{sinc}(n\varphi_0/2)}{\epsilon_n} \dot{w}_n(z/a) \cos(n\varphi). \tag{16}$$

The pipe radial velocity distribution along the z-axis is shown in Figure 4, plotted in a non-dimensional way as $\rho_s \epsilon_s \pi a h \epsilon_n |\dot{w}_n(z/a)|/F_0$. Due to the interference between modes with same circumferential distributions but different axial wavelengths, the magnitude of the radial velocity fluctuates with distance.

When the non-dimensional frequency Ω is less than 0·6, the magnitude of the transfer mobility of any mode n is basically independent of distance, since there is only one

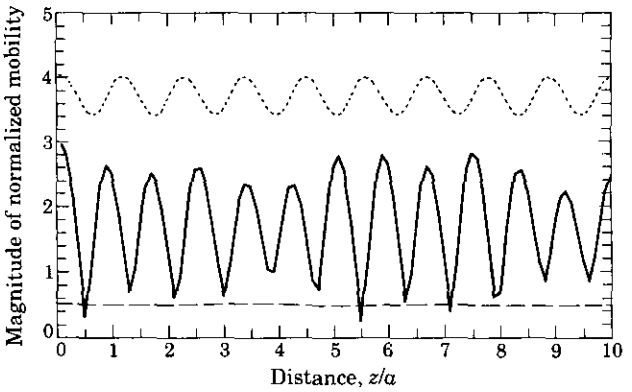

Figure 4. The shell radial velocity distribution along the axial distance, $h/a = 0{\cdot}05$. Expressed in a normalized way as $\rho_s c_s \pi a h \epsilon_n |\dot{w}_n(z/a)|/F_0$. – – –, Water-filled pipe, $n = 0$, $\Omega = 0{\cdot}5$; ——, water-filled pipe, $n = 0$, $\Omega = 1{\cdot}5$; · · · · ·, pipe *in vacuo*, $n = 1$, $\Omega = 1{\cdot}2$.

travelling wave for any $n \neq 0$ mode. For the $n = 0$ mode, there are two travelling waves (the purely torsional wave is not included since it is uncoupled from other modes), but the response of the fluid mode to radial excitation is much higher than that of the shell mode [12] and the total response is dominated by that of the fluid mode. At higher frequencies, the magnitude of the total response of any mode n varies periodically with axial distance, since there are two or more different travelling waves with the same circumferential distributions and comparable responses. The magnitude of the fluctuation depends on the differences between the magnitudes, and the period of the fluctuation depends on the differences between the axial wavenumbers. Even the pipe vibrating *in vacuo* shows the same interference pattern when there are two or more travelling waves with the same circumferential distributions (the dotted line in Figure 4). Note that there is no interference between different modes n if circumferential averaging is taken.

4.2. SOUND POWER

The sound power radiated by a unit length of the pipe also varies with the axial distance, due to the distribution of the pipe radial velocity. The pipe concerned is assumed to be in air, the density of which is much smaller than that of the shell and of the fluid inside. By using the shell radial velocity obtained previously, the sound pressure can be expressed as

$$p^a(r, \varphi, z) = -\mathrm{j}\rho_a \omega \sum_{n=0}^{\infty} \cos(n\varphi) \sum_{m=1}^{K_n} \frac{H_n^{(2)}(\alpha_{nm}^a r)}{\alpha_{nm}^a \mathrm{H}_n^{(2)\prime}(\alpha_{nm}^a a)} \dot{w}_{nm} \mathrm{e}^{-\mathrm{j}k_{nm} z}, \tag{17}$$

where the subscript and superscript a denotes "air", $\mathrm{H}_n^{(2)}$ is the Hankel function of the second kind (order n) and α_{nm}^a is the radial wavenumber of the mode (n, m) in air.

The sound power radiated by a unit length of the pipe is the integral of the r-direction sound intensity on the pipe surface over the circumferential direction:

$$T^a = \int_0^{2\pi} \frac{1}{2} \mathrm{Re}\,(p^a \dot{w}^*(\varphi, z))|_{r=a}\, a\, \mathrm{d}\varphi. \tag{18}$$

Upon using the orthogonality of the sinusoidal functions and applying the relation

$$-\mathrm{j}\mathrm{H}_n^{(2)}(x)\mathrm{H}_n^{(1)\prime}(x) = \frac{2}{\pi x} - \mathrm{j}[\mathrm{J}_n(x)J_n'(x) + \mathrm{Y}_n(x)Y_n'(x)], \tag{19}$$

the integral can be evaluated as

$$T^a = \sum_{n=0}^{\infty} T_n^a = \sum_{n=0}^{\infty} (T_{n1}^a + T_{n2}^a + T_{n3}^a). \tag{20}$$

In this expression,

$$T_{n1}^a = \frac{\epsilon_n \pi a \rho_a c_a}{2} \sum_{m=1}^{K_n} \sigma_{nm} |\dot{w}_{nm}|^2 \tag{21}$$

is the axially averaged sound power radiated by a unit length of the pipe and σ_{nm} is the radiation efficiency of mode (n, m). The interference terms are

$$T_{n2}^a = \frac{\epsilon_n \pi a \rho_a c_a}{2} \sum_{m=2}^{K_n} \sum_{l=1}^{m-1} (\sigma_{nm} + \sigma_{nl}) |\dot{w}_{nm}| |\dot{w}_{nl}| \cos [(k_{nm} - k_{nl})z + \psi_{ml}] \tag{22}$$

and

$$T_{n3}^a = -\frac{\epsilon_n \pi a \rho_a c_a}{2} \sum_{m=2}^{K_n} \sum_{l=1}^{m-1} (g_{nm} - g_{nl}) |\dot{w}_{nm}| |\dot{w}_{nl}| \sin [(k_{nm} - k_{nl})z + \psi_{ml}], \tag{23}$$

with

$$g_{nm} = \sigma_{nm} \frac{\pi(\alpha_{nm}^a a)(\mathrm{J}_n(\alpha_{nm}^a a)\mathrm{J}_n'(\alpha_{nm}^a a) + \mathrm{Y}_n(\alpha_{nm}^a a)\mathrm{Y}_n'(\alpha_{nm}^a a))}{2}, \tag{24}$$

where ψ_{ml} is the phase difference of mode (n, m) and (n, l) at point $z = 0$.

T_{n1}^a is the sum of the contributions of all modes when each of them exists individually, and T_{n2}^a is the fluctuation of sound power due to structural wave interference *within* the shell. The axial distribution of the sum of T_{n1}^a and T_{n2}^a is the same as that of the pipe radial displacement. T_{n3}^a is the result of acoustic wave interference due to the non-uniform distribution of the pipe displacement. Calculations [12] show that T_{n3}^a is much smaller than T_{n2}^a and can be neglected, as one expected. If averaged over a long distance, both T_{n2}^a and T_{n3}^a tend to zero.

When two travelling waves with the same distribution $\cos(n\varphi)$ satisfy the condition $(k_{n1} - k_{n2})z + \psi_{12} = k\pi$ at the point z, the second term of sound power reaches its maximum while the third vanishes, since the fluctuation of the shell displacement reaches its maximum and the vibrational pattern is symmetrical about this point. Conversely, when $(k_{n1} - k_{n2})z + \psi_{12} = (2k + 1)\pi$, the second term vanishes and the third maximizes, since the fluctuation of the shell displacement is zero and the vibration surface is asymmetrical about this point.

By using the real part of the non-dimensional input mobility, $RM_{nm} = \mathrm{Re}(\dot{w}_{nm} \rho_s c_s \pi a h \epsilon_n / F_0)$, the averaged sound power under a point force excitation can be expressed as

$$T_1^a = \sum_{n=0}^{\infty} T_{n1}^a = \frac{\rho_a c_a}{2\pi a} \left(\frac{F_0}{\rho_s c_s h} \right)^2 \sum_{n=0}^{\infty} \frac{1}{\epsilon_n} \sum_{m=1}^{K_n} \sigma_{nm} RM_{nm}^2. \tag{25}$$

If a wide-band force is applied instead of a harmonic one, the only change in equation (25) is to use $T_1^a(\omega)$ and $S_{ff}(\omega)$ to replace T_1^a and $F_0^2/2$, where $S_{ff}(\omega)$ is the power spectral density of the applied force.

In Figure 5, is shown the relative fluctuation of the sound power, $(T_{n2}^a + T_{n3}^a)/T_{n1}^a$, of the $n = 1$ mode. The observation point is assumed to be at $z = 100a$. Fluctuations at certain frequencies can be very high, even up to 80 per cent. If averaged axially over a distance of five radii, the fluctuation becomes small (the solid line in Figure 5), but is still detectable in certain frequency regions.

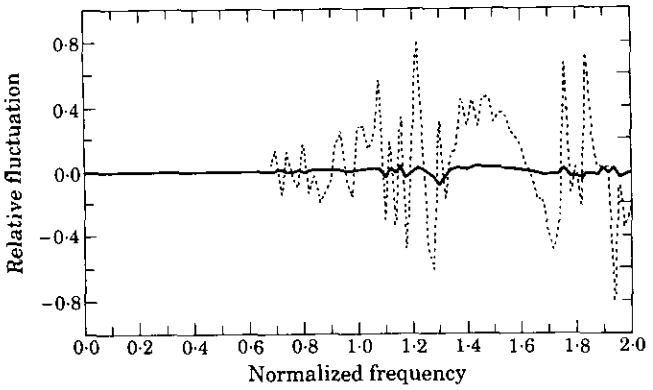

Figure 5. The relative fluctuation of the sound power $(T^a_{n2} + T^a_{n3})/T^a_{n1}$. Water-filled pipe, $h/a = 0{\cdot}05$, $n = 1$ mode. · · · · · , At $z = 100a$; ——, axially averaged over five radii of the pipe.

Fuller [5] also observed that radiated sound power, excited by a monopole in the air inside the pipe, is characterized by a harmonic oscillation with axial distance when the source location is $r_p/a = 0$. He interpreted the phenomenon by using the "surface power" concept. In reference [5], the calculation is at very low frequency ($\Omega = 0{\cdot}05$), and hence the fluctuation of sound power can be observed only for axisymmetric excitation, since there is only one travelling wave for each higher order n mode. If the frequency is increased, say $\Omega = 1{\cdot}5$, the fluctuation of the sound power along the axial distance will be observed for any source distribution.

From the discussion of this section it can be seen that the mechanism of the sound power fluctuation is the interference of structural and acoustic waves, mainly of the structural waves. To interpret this phenomenon, it is better to use directly the concept of structural wave interference.

5. COUPLING EFFECTS

Influences of the coupling parameter η on the system response have been analyzed by varying the density ratio ρ_f/ρ_s and the thickness ratio h/a separately [12]. In Figure 6 are shown the responses of the first five circumferential distributions of the water-filled pipe compared with the corresponding *in vacuo* results. (Note that there might be more than

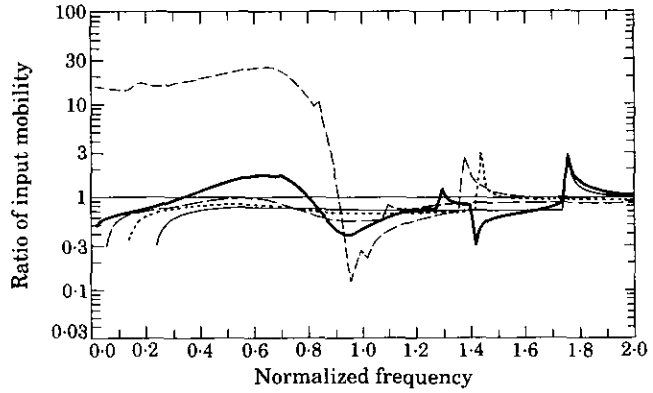

Figure 6. A comparison of the responses of the water-filled pipe with *in vacuo* results; $h/a = 0{\cdot}05$. - - - , $n = 0$; ——, $n = 1$; – – – , $n = 2$; · · · · · , $n = 3$; — · —, $n = 4$.

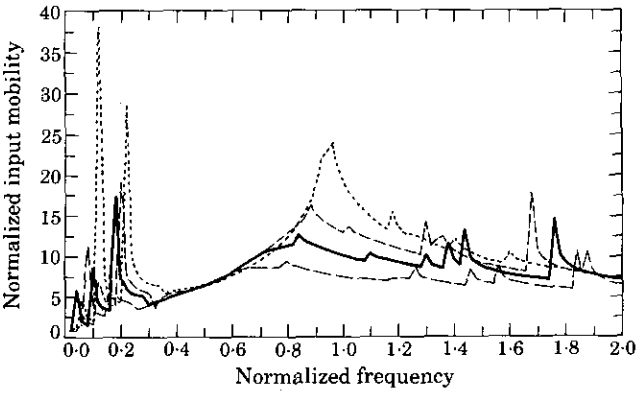

Figure 7. The influence of the density ratio on the shell radial response, distributed force excitation, plotted in $\rho_s c_s \pi a h \dot{w}(0,0)/F_0$. Fluid-filled pipe, $h/a = 0{\cdot}05$, force distribution angle $\varphi_0 = 0{\cdot}9$. · · · · ·, $\rho_f/\rho_s = 0{\cdot}0128$; - - -, $\rho_f/\rho_s = 0{\cdot}064$; ——, $\rho_f/\rho_s = 0{\cdot}128$; – – –, $\rho_f/\rho_s = 0{\cdot}256$.

one axial mode for each circumferential distribution.) For any distributions with $n \geqslant 2$, coupling with the fluid reduces responses for all frequencies. When the normalized frequency Ω is higher than 1, the coupling also reduces responses for the $n = 1$ and $n = 0$ modes. However, when Ω is less than 1, the coupling increases the response of the $n = 0$ mode, since the main responding mode is a fluid mode in that frequency region. The smaller the density ratio, the more concentrated and the more sharp is the axisymmetric response. For the $n = 1$ mode, the coupled system has a lower response when the frequency is below about $\Omega = 0{\cdot}3$. Then, in the frequency region of about $\Omega = 0{\cdot}3$ to $\Omega = 0{\cdot}7$, the situation is reversed. After that, the system with stronger coupling again has a lower response. By a comparison with Figure 2(c) it can be seen that just in the frequency region of about $\Omega = 0{\cdot}3$ to $\Omega = 0{\cdot}7$, the main responding mode for the $n = 1$ (i.e., (1, 1)) mode, is a fluid mode.

Comparisons of the system responses to distributed force excitations are shown in Figure 7. The force is assumed to have the form of equation (14) with tangential distribution angle $\varphi_0 = 0{\cdot}9$ and axial distribution length $B = 0$. The summation of equation (16) is truncated at $n = 7$: that is, only the terms satisfying the condition $n < 2\pi/\varphi_0$ are considered. The low frequency ($\Omega < 0{\cdot}4$) responses are complicated, since the total response of the system is dominated by a series of cut-on resonant peaks. The effects of coupling on the radial response are very dependent on the frequency concerned. However, in general, the averaged response is reduced when coupled with a dense fluid. At high frequencies ($\Omega > 0{\cdot}7$), coupling with a dense fluid suppresses the radial response. For middle frequencies, there is no significant response reduction. Instead, there is even a small increase at $\Omega \sim 0{\cdot}55$ when coupled with a dense fluid. This is because, in this frequency region, the responses of both $n = 0$ and $n = 1$ modes are increased for a coupled system, and there is no significant reduction for the $n = 2$ mode. In this frequency region, it cannot be determined if coupling increases or decreases the response before the excitation is assessed.

Frequency characteristics of four different combinations of parameters, shown in Table 2, are compared. The radial responses of the $n = 1$ mode are shown in Figure 8(a). The situations for all other modes are similar. At low frequencies ($\Omega < 0{\cdot}4$), the frequency dependences are almost exactly the same if different groups have the same coupling parameter η. The only differences are the cut-on frequencies of high n-modes, which increase with thickness ratio h/a. At high frequencies, the frequency dependences of modal

TABLE 2

Different combinations of parameters

Group	Thickness ratio, h/a	Density ratio, ρ_f/ρ_s	Coupling parameter, η	$\eta(h/a)^2$
A	0·1	1/7·8	1·28	1·28E − 2
B	0·05	0·5/7·8	1·28	3·2E − 3
C	0·025	1/7·8	5·12	3·2E − 3
D	0·05	2/7·8	5·12	1·28E − 2

responses are similar if the systems have the same $\eta(h/a)^2$, but the positions of the resonant peaks depend only on the coupling parameter η.

This phenomenon can be interpreted as follows. At low frequencies, the principle wave motions are axial and tangential. The main part of response is the term without the factor $\beta^2 = h^2/12a^2$. The factor which determines these terms is the coupling parameter η. At high frequencies, bending waves dominate; the terms with β^2 are the main parts of response. Hence systems with the same $\eta\beta^2$ display roughly the same responses. Resonant peaks at high frequencies usually correspond to the cut-on of fluid modes, which depends to a great extent on the coupling parameter η. Systems with the same coupling parameter η have the same cut-on frequencies of fluid modes, and have the same positions of the resonant peaks. However, the first mode of each circumferential distribution $n > 1$ is always a shell mode, and its cut-on frequency also depends, on the thickness ratio. Comparisons have been made only for a certain range of thickness and density ratios. With an extremely thin or thick wall, the situation may be different.

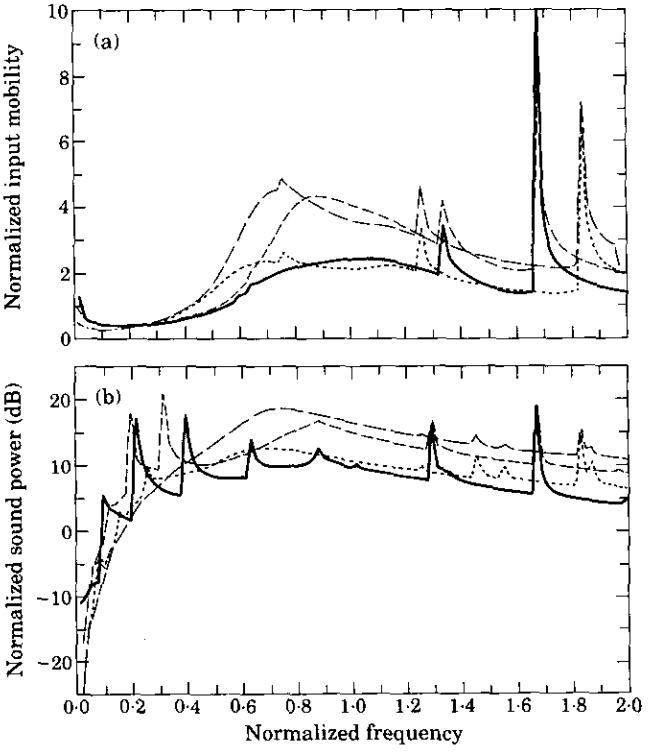

Figure 8. A comparison of different combinations of thickness ratio and density ratio. (a) Single mode response $\rho_s c_s \pi a h \epsilon_n \dot{w}_n(0)/F_0$; (b) sound power $2\pi a(\rho_s c_s h/F_0)^2/\rho_a c_a T_1^a$. ——, A; - - -, B; – – –, C; · · · · ·, D.

The total responses of the same systems to a distributed force excitation have also been examined. The force applied is the same as that for Figure 7. Unlike that of an individual mode, the frequency dependencies of total responses are different at low frequencies for systems with the same coupling parameter but different thickness ratios, due to a series of cut-on resonances, as explained previously. However, the frequency dependence of the total noise power (see Figure 8(b)) again shows the same frequency characteristics as those for individual modes. This is because that when a mode is newly cutting on, $\alpha_{nm}^{a}a$ is much smaller than the circumferential number n. The "wavelength" in the circumferential direction is much smaller than the wavelength in air. The radiation efficiency is very low for such a mode, even though it is a supersonic wave [11]. Thus all cut-on resonances are suppressed to a certain extent. Note that in Figure 8 only the frequency properties of the systems are compared. A normalization factor, which includes pipe radius and thickness, is omitted. If this factor is taken into account, the absolute value of the noise power is different for systems with different pipe thickness.

A pipe with a thinner wall usually has a higher radial response for the same excitation. However, this is not always true for noise, where power radiated by a very thin wall is sometimes smaller than that by a thicker one; see Figure 9. For the purpose of examining the influence of thickness on the absolute value of noise power, Figure 9 is normalized differently from other parts of the paper: i.e., $2\pi a^3(\rho_s c_s/F_0)^2/\rho_a c_a T_1^a$ is plotted. This means that the comparisons are for pipes with the same diameter but different thicknesses. In the frequency region $\Omega \in (0{\cdot}62, 1{\cdot}66)$, there is a sharp drop in the sound power when $h/a = 0{\cdot}01$, although the shell radial velocity is still the highest among those compared. The reason is that both (0, 1) and (1, 1) modes are subsonic in this frequency region, since all of the other important acoustic modes are subsonic already. Thus a very thin wall does not always radiate more noise than a thicker wall at middle and high frequencies for a fluid-filled pipe. Obviously, this behavior is independent of the excitation, since the mechanism is that all acoustically important modes are subsonic. This is a new phenomenon, for a pipe coupled with interior fluid. Such a situation never arises for a pipe vibrating in air.

5.1. INFLUENCES OF FORCE DISTRIBUTION

The influences of the force distribution on radiated sound power are illustrated in Figure 10. The force applied is expressed by equation (14) and the results are plotted in

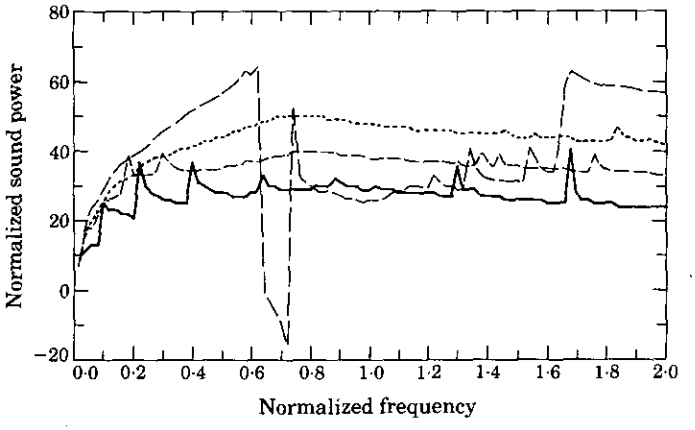

Figure 9. The influence of the thickness ratio on the radiated sound power; water-filled pipe, density ratio $\rho_f/\rho_s = 0{\cdot}128$. ——, $h/a = 0{\cdot}1$; - - -, $h/a = 0{\cdot}05$; · · · ·, $h/a = 0{\cdot}025$; — — —, $h/a = 0{\cdot}01$. The sound power is plotted as $2\pi a^3(\rho_s c_s/F_0)^2/\rho_a c_a T_n^a$.

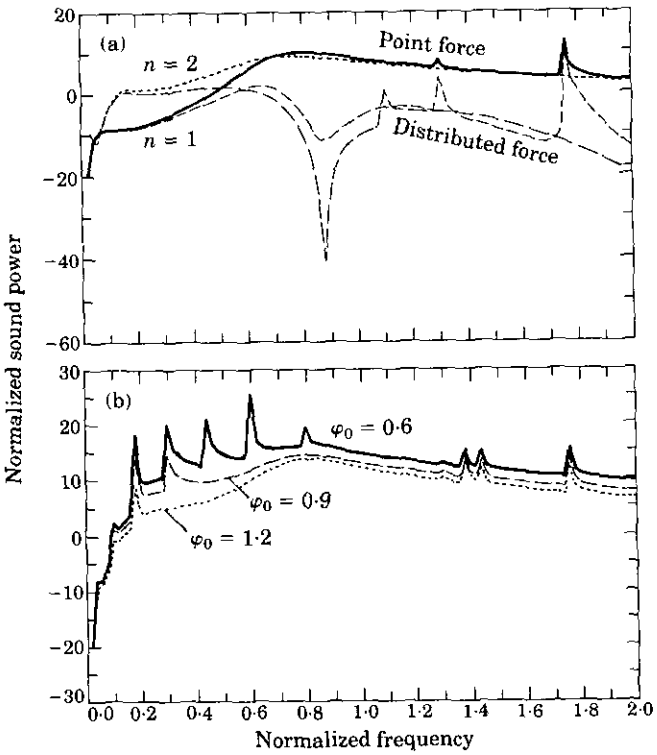

Figure 10. The influence of the force distribution: thickness ratio $h/a = 0{\cdot}05$, density ratio $\rho_f/\rho_s = 1/7{\cdot}8$. (a) Axial distribution, the distribution length equals the radius; (b) circumferential distribution.

a normalized way. The total force applied is the same for all cases. In Figure 10(a) are shown the noise powers of individual n modes when the force axial distribution length B equals zero or equals the pipe radius, respectively. It is clear that the influence of the force axial distribution is mainly at middle and high frequencies, when the wavelength of the main radiation mode is close to, or shorter than, the length of the force distribution. If the non-dimensional frequency Ω is greater than 0·7, an axial force distribution over a length of the pipe radius could reduce the noise power by 10–20 dB. Hence, to have force distributed over a long distance in the axial direction is always helpful in noise control problems.

The effect of the distribution in the tangential direction is similar, but not significantly. In Figure 10(b) are shown the sound powers radiated by a unit length of the pipe when the force has different circumferential distributed angles φ_0. In this case the axial distribution length is equal to zero. At very low frequencies ($\Omega < 0{\cdot}2$), the force distribution has almost no effect on radiated sound power, as in the case of an axial force distribution. At high frequencies ($\Omega > 0{\cdot}8$), the power is doubled when the angle of the force distribution is halved. The force distribution in the φ direction shows radical noise reduction only at middle frequencies ($\Omega \in (0{\cdot}2, 0{\cdot}8)$), where a wide distribution suppresses the high order n modes, which are the most important modes in this frequency region. Hence for the purpose of noise control, the force applied should be distributed in the φ direction if the noise is mainly at middle frequencies, and in the axial direction if the noise is at high frequencies.

6. CONCLUSIONS

There is no simple relationship between the radiated sound power and the power distribution within the coupled system. However, the power distribution is affected if the coupling increases or decreases the pipe response to external radial force excitation, and noise power. If the power in the coupled system is propagating mainly in the fluid, coupling will increase the pipe response. Otherwise, coupling will reduce the response. Both pipe radial displacement and the radiated sound power fluctuate with the axial distance if the frequency is high enough. This is due to the interference of travelling waves with the same circumferential distribution but different axial wavenumbers. This phenomenon happens even if there is no coupling with the interior fluid.

Coupling with the fluid usually reduces the pipe radial response and the radiated noise power at low and high frequencies. In a certain region of the middle frequencies, coupling may increase the radial response, and hence the noise power, if the $n = 1$ mode dominates. Otherwise, the opposite applies. Distributing the force over a large area is helpful in noise and vibration control.

REFERENCES

1. C. R. FULLER and F. J. FAHY 1982 *Journal of Sound and Vibration* **81**, 501–518. Characteristics of wave propagation and energy distributions in cylindrical elastic shells filled with fluid.
2. G. PAVIC 1990 *Journal of Sound and Vibration* **142**, 293–310. Vibrational energy flow in elastic circular cylindrical shells.
3. G. PAVIC 1990 *3rd International Congress on Intensity Techniques, Senlis*, France, 159–166. Energy flow through straight pipes.
4. C. R. FULLER 1983 *Journal of Sound and Vibration* **87**, 409–427. The input mobility of an infinite circular cylindrical elastic shell filled with fluid.
5. C. R. FULLER 1986 *Journal of Sound and Vibration* **109**, 259–275. Radiation of sound from an infinite cylindrical elastic shell excited by an internal monopole source.
6. C. R. FULLER 1988 *Journal of Sound and Vibration* **122**, 479–490. Sound radiation from an infinite elastic cylinder with dual-wave propagation—intensity distribution.
7. W. FLÜGGE 1973 *Stress in Shells*. New York: Springer-Verlag.
8. C. R. FULLER 1984 *Journal of Sound and Vibration* **96**, 101–110. Monopole excitation of vibrations in an infinite cylindrical elastic shell filled with fluid.
9. P. M. MORSE and K. U. INGARD 1968 *Theoretical Acoustics*. New York: McGraw-Hill.
10. A. J. ROMANO, P. B. ABRAHAM and E. G. WILLIAMS 1990 *Journal of the Acoustical Society of America* **87**, 1166–1175. A Poynting vector formulation for thin shells and plates, and its application to structure intensity analysis and source localization, part I: theory.
11. L. CREMER, M. HECKL and E. E. UNGAR 1988 *Structure-Borne Sound* Berlin: Springer-Verlag; second edition.
12. L. FENG 1991 *Royal Institute of Technology, Stockholm, Sweden, Report TRITA-TAK* 9105. Structure response and acoustic radiation of an infinite cylindrical shell filled with fluid.

APPENDIX A: STRUCTURE POWER FOR A SINGLE TRAVELLING MODE

The force and moments in equation (6) are of the forms

$$Q_z = \int_{-h/2}^{h/2} \tau_{zr}(1 + x/a)\,\mathrm{d}x, \qquad N_{z\varphi} = \int_{-h/2}^{h/2} \tau_{2\varphi}(1 + x/a)\,\mathrm{d}x, \qquad N_z = \int_{-h/2}^{h/2} \sigma_z(1 + x/a)\,\mathrm{d}x, \tag{A1–A3}$$

$$M_{z\varphi} = \int_{-h/2}^{h/2} \tau_{z\varphi} x(1 + x/a)\,\mathrm{d}x, \qquad M_z = \int_{-h/2}^{h/2} \sigma_z x(1 + x/a)\,\mathrm{d}x. \tag{A4, A5}$$

After integrating, and neglecting some least important terms for a thin shell, the simplified Flügge relations, expressed in terms of the middle surface displacement, are obtained as

$$Q_z = -\frac{1}{a}\frac{\partial M_{\varphi z}}{\partial \varphi} - \frac{\partial M_z}{\partial z} = -\frac{D(1-\nu)}{a^2}\frac{\partial^3 w}{\partial^2 \varphi\, \partial z} - D\left(\frac{\partial^3 w}{\partial z^2 \partial \varphi} + \frac{\nu}{a^2}\frac{\partial^3 w}{\partial \varphi^3}\right), \tag{A6}$$

$$N_{z\varphi} = \frac{B(1-\nu)}{2}\left(\frac{1}{a}\frac{\partial u}{\partial \varphi} + \frac{\partial v}{\partial z}\right), \qquad N_z = B\left(\frac{\partial u}{\partial z} + \frac{\nu}{a}\frac{\partial v}{\partial \varphi} + \frac{\nu}{a}w\right), \qquad N_{z\varphi} = \frac{D(1-\nu)}{a}\frac{\partial^2 w}{\partial \varphi\, \partial z},$$

$$M_z = D\left(\frac{\partial^2 w}{\partial z^2} + \frac{\nu}{a^2}\frac{\partial^2 w}{\partial \varphi^2}\right), \tag{A7–A10}$$

where

$$B = Eh/(1-\nu^2), \qquad D = Eh^3/12(1-\nu^2) \tag{A11, A12}$$

are the membrane stiffness and bending stiffness, respectively. By using these expressions and equation (6), the final expression (8) is obtained after averaging over time and integrating over the φ direction. Note that the simplified Flügge equations are used here instead of the exact ones, since they are consistent with the governing equation (the simplified Flügge equation).

APPENDIX B: LIST OF SYMBOLS

a	radius of the middle surface of pipe; superscript for "air"	Re ( )	take real part of the expression
		RM	real part of non-dimensional input mobility
c_a	acoustic free wave speed in air		
c_f	acoustic free wave speed in fluid	T	energy flow; sound power
c_s	plate extensional wave speed	w, v, u	displacements in r, φ and z direction
E	Young's modulus	x_{nm}	$=\alpha_{nm}a$, non-dimensional radial wavenumber of mode (n, m)
f	subscript and superscript for "fluid"		
f_r, f_φ, f_z	external forces	y_{nm}	$=k_{nm}a$, non-dimensional axial wavenumber of mode (n, m)
FL	fluid loading term		
g_{nm}	acoustic interference factor	z	axial co-ordinate
h	thickness of pipe wall	α_{nm}	radial wavenumber
$H_n^{(2)}$	Hankel function of the second kind, of order n	β^2	thickness factor
		ϵ_n	$=2$ if $n=0$, $=1$ if $n>0$
J_n	Bessel function of order n	η	coupling parameter
k_{nm}	axial wave number of mode (n, m)	ρ_a	density of air
L_1, L_2	polynomials; see equations (4) and (5)	ρ_f	density of fluid inside the pipe
m	axial mode index	ρ_s	density of the pipe material
M_z	bending moment	Γ	power ratio
$M_{z\varphi}$	shear moment	ν	Poisson ratio
n	circumferential mode index	ω	circular frequency
N_z	axial force in pipe	Ω	$=\omega a/c_s$, normalized frequency
$N_{z\varphi}$	torsional shear force in pipe	$\dot{()}$	differentiation with respect to time
p	acoustic pressure	$()'$	differentiation with respect to non-dimensional parameter
P	unit width shell energy flow		
Q_z	transverse shear force in pipe	$(*)$	complex conjugate
r	radial co-ordinate		